CHEMISTRY
A EUROPEAN JOURNAL

DOI: 10.1002/chem.200600293

Shape-Controlled Synthesis of Zinc Oxide: A Simple Method for the Preparation of Metal Oxide Nanocrystals in Non-aqueous Medium

Zhihua Zhang,[a] Meihua Lu,[b] Hairuo Xu,[a] and Wee-Shong Chin*[a]

Abstract: A general and facile approach has been developed to prepare various metal oxide nanocrystals from commercially available metal acetate precursors using an amine-mediated reaction. The influence of temperature and capping agents on the yield and final morphology of the metal oxides nanocrystals was investigated. The approach was applied in the synthesis of shape-controlled ZnO nanocrystals. ZnO nanowires, nanorods, bullets and triangular nanocrystals were successfully prepared by tuning the molar ratio between amine to zinc acetate precursor. On the basis of FTIR and NMR spectroscopic studies, we propose that the amine could mediate the breakdown of the metal acetates through a nucleophilic attack mechanism. The results suggest that amine can play dual role as both the attacking agent and capping agent in this new methodology.

Keywords: nanostructures · nanotechnology · nanowires · zinc oxide

Introduction

Nanocrystalline metal oxides have found applications in many technologies including solar energy conversion,[1] ductile ceramics,[2] superconductors,[3] chemical sensors,[4] magnetic devices.[5] Due to their promising perspectives in these myriad areas, many approaches including both physical and chemical strategies have been developed for the preparation of these nanomaterials. Among the various techniques developed to prepare metal oxide nanomaterials, chemical colloidal methods are of particular interests as they allow facile scale-up and convenient control of particle sizes and morphologies. Basically, chemical methods could be divided into two major approaches: hydrolytic and nonhydrolytic methods. For hydrolytic methods, traditional chemical routes involve firstly the solubilization of an inorganic or organometallic salt in an aqueous or alcoholic solvent; this is followed by hydrolysis using strong hydrolyzing agents such as NH_4OH or NaOH.[6] In most case, the nanomaterials thus obtained are amorphous and are covered with a surface layer of hydroxylated groups that can adversely affect the properties of these materials. Hence, follow-up treatments such as calcinations are needed in order to produce the desired properties.

In order to overcome some of the drawbacks, extensive efforts have been put into finding nonhydrolytic synthesis methods of metal oxides. Halide elimination method is one of such special routes to prepare metal oxides by reacting metal chlorides with alcohols, alkoxides or ethers. However, environmentally unfriendly gases such as alkyl chlorides or hydrogen chlorides are released during the process.[7] Recently, magnetic oxides nanocrystals such as iron oxide and metal ferrite have been synthesized from high-temperature reaction of metal acetylacetonate.[8] Other analogous compounds have also been used for the preparation of other transition metal oxides nanocrystals.[9] Decomposition of metal complexes,[10] as well as oxidation of metal organometallic compound such as organic alkyl metal precursors and metal carbonyl, has also been utilized for the preparation of oxide nanocrystals.[11] On the other hand, the ether elimination process,[12] aminolysis route[13] and cleavage between carbon bonds[14] have also been explored to prepare metal oxides nanomaterials with tunable sizes and morphologies.

In this manuscript, we report a simple and generalized method to prepare metal oxide nanocrystals from metal acetates. In our search for organometallic complexes that can be used as precursors for the preparation of oxide nanocrystals, we have found that metal acetates can readily react with amines in general to give the corresponding metal oxides under suitable conditions. The possibility of using

[a] Z. Zhang, H. Xu, Dr. W.-S. Chin
Department of Chemistry, National University of Singapore
3 Science Drive 3, Singapore 117543 (Singapore)
Fax: (+65) 6779-1691
E-mail: chmcws@nus.edu.sg

[b] M. Lu
Department of Materials Science, National University of Singapore
3 Science Drive 4, Singapore 117543 (Singapore)

Supporting information for this article is available on the WWW under http://www.chemeurj.org/ or from the author.

commercially available metal acetates for the generation of metal oxides is exciting. In comparison, this method is of relatively low cost, easy to manipulate and can be readily scaled up for industrial production. In particular, we illustrate in detail our approach to obtain shape-specific ZnO nanocrystals in unique triangular and rod shape using this general approach. ZnO is one of the most important functional materials for its unique properties in near-UV emission and optoelectronic applications. As far as we are aware, non-aqueous synthesis of ZnO nanoparticles has only been reported via the oxidation or decomposition of alkylzinc precursor and organic zinc compounds.[10b,c,f,g,11a,c,d]

Results and Discussion

By varying the experimental conditions such as temperature, reaction time, reagent ratios and the type of amine used, ZnO nanocrystals of uniform sizes and various morphologies have been obtained using our proposed methodology. The morphologies and sizes of ZnO nanocrystals are summarized in Table 1. In the following discussion, the effect of various experimental parameters will be illustrated in details first, followed by discussion on the possible reaction mechanism and its generalization.

Table 1. Summary of various sizes and morphologies of ZnO nanocrystals prepared from zinc acetate at different reaction conditions.

Amine[a]	Amine-to-$Zn(Ac)_2$ ratio	Reaction time [min]	T [°C]	Size		Morphology
				Diameter [nm]	Length [nm]	
OLA	1	20	240	22 ± 2.4	500–2000	nanorods
OLA	2	20	240	35 ± 4.3	200–600	nanorods
OLA	3	20	240	51 ± 13	100–200	bullet-like crystals
OLA	2	20	320	62.5 ± 12	150–350	nanorods
OLA	2	60	180	39 ± 4.6	100–320	nanorods
OLA	4	20	240	–	85 ± 12	prism
OLA	24	60	240	–	71 ± 11	prism
DOA	2	20	240	26 ± 3.1	500–1500	nanowires
HDA	2	20	240	37 ± 4.2	200–600	nanorods
DDA	2	20	240	50 ± 6.2	100–150	nanorods

[a] OLA = oleylamine, HDA = hexadecylamine, DOA = dioctylamine, DDA = dodecylamine.

We have found that the variation of the relative amine-to-precursor molar ratios affords a very convenient way to control the morphology of the ZnO nanocrystals. Thus, while nanorods are formed when the amine-to-precursor ratio is ~1:2, uniform triangularly shaped ZnO nanoparticles are produced at higher amine ratios. Typical TEM images in Figure 1 show the morphology and size of the ZnO nanocrystals prepared from oleylamine (OLA) at different molar ratios.

In Figure 1a, bundles of long and thin ZnO nanowires with diameter about 20 nm and length of 500–2000 nm are observed. By simply increasing the OLA-to-acetate ratio to 2, thicker and shorter nanorods (ca. 35 nm × 200–600 nm) were obtained such as depicted in Figure 1b. Interestingly, increasing the amount of OLA further to 3 mmol produces bullet-like ZnO nanocrystals as shown in Figure 1c. Finally, triangularly shaped ZnO nanocrystals were almost exclusively formed when the amount of OLA was increased to 4 mmol. An excess amount of OLA of up to 24 mmol (Table 1) was found to have no further effect on the morphology as triangular nanocrystals were obtained as the only form in the isolated product.

Figure 2 shows typical XRD patterns for the as-synthesized ZnO nanocrystals prepared from OLA. The diffraction patterns clearly show the excellent crystallinity of the samples obtained. All peaks can be indexed to the hexagonal wurtzite structure of ZnO. The crystal lattices of $a = b = 3.25$ and $c = 5.21$ Å determined from XRD fit well with values in the database (JCPDS, 36-1451). Comparatively, the intensity of the (002) peak in ZnO nanowires is slightly higher than that of the triangular crystals. This could suggest that the nanowires grow preferentially along the c axis. It is noted that currently reported chemical approaches such as hydrothermal or sol–gel methods have rarely produced uniform ZnO nanocrystals ranging from tens of nanometers to micrometer in terms of diameter and length. In our case, the diameters of the nanocrystals are rather uniform although the length homogeneity is less easy to control.

In Figure 3, a correlation between the aspect ratios (length/width) as well as the diameter (or width) of the ZnO nanocrystals against the molar ratio of amine is clearly illustrated. Thus, we may conclude that increasing the amount of amine enhances the growth in the a and b axes but weakens the growth along the c axis.

We have found that the temperature also has some effect on the growth of the nanorods (Table 1). Thus, using OLA at molar ratio of 2, nanorods with average diameter of 39 nm and length of 100–320 nm were obtained at 180 °C. At 320 °C, on

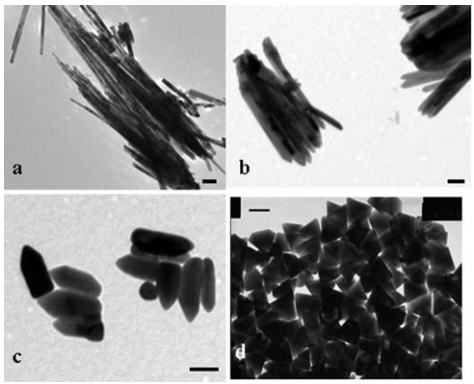

Figure 1. TEM images of various ZnO nanocrystals obtained from $Zn(Ac)_2$ reacted with OLA at 240 °C using different OLA/acetate molar ratio: a) 1, b) 2, c) 3, and d) 4. All scale bars = 100 nm.

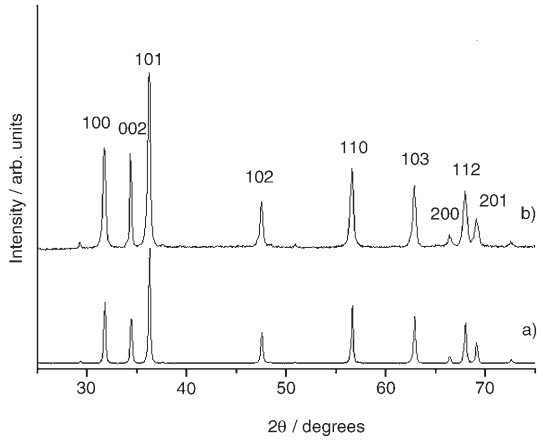

Figure 2. XRD patterns of different ZnO nanocrystals prepared from $Zn(Ac)_2$ reacted with OLA: a) triangular nanocrystals (OLA/acetate = 4) and b) ZnO nanowires (OLA/acetate = 1).

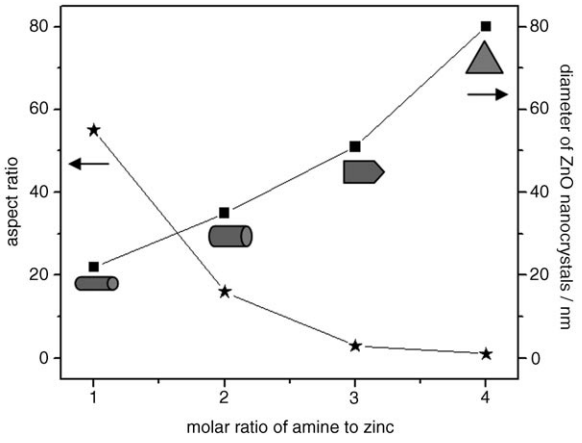

Figure 3. Correlation plot showing the relationship of aspect ratio and diameter of ZnO nanocrystals against the molar ratio of OLA-to-acetate in the reaction.

the other hand, thicker nanorods (63 nm × 150–350 nm) were produced. Both of these nanorods have relatively lower aspect ratio as compared to that obtained at 240 °C with the same reaction mixture. Thus, optimizing the temperature is also important for tuning the aspect ratio of the produced ZnO nanorods.

Next we attempted to analyze the morphology of the nanorods (see Figure 4) and triangles in more detail. A single ZnO nanorod with a diameter of 22 nm is shown in Figure 4a; the corresponding SAED pattern is depicted in Figure 4b. It is thus confirmed that the obtained nanorods exhibit a single-crystalline structure and grow in the [0001] direction. The HRTEM image in Figure 4c reveals a lattice spacing of 0.26 nm, which corresponds well to the *d* spacing of the (002) planes of hexagonal ZnO. For the triangular ZnO nanocrystals (Figure 4d), lattice spacing of 0.26 nm was also observed, suggesting that these triangles are made up of faces dominated with the (002) planes. In Figure 4e and f, abundant quantity of ZnO nanorods and triangular nanocrystals are shown in SEM. The estimated length of the nanorods ranges from 400 to 1600 nm, while their diameter is less easy to be determined since they were bundled together. This coplanar bundling aspect will be discussed below. Careful SEM analysis reveals that the triangular nanocrystals may be more accurately described as regular tetrahedral prisms with length of ~70–80 nm on each side.

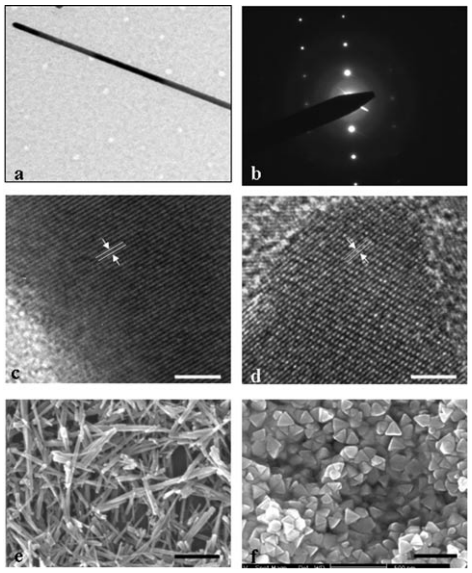

Figure 4. a), b) TEM image and SAED pattern of a free-standing ZnO nanorod; c), d) HRTEM of the ZnO nanorod and triangular ZnO nanocrystal, respectively. Scale bar = 5 nm; e), f) SEM image of the ZnO nanorods and triangular nanocrystals. Scale bar = 500 nm.

We further investigated the effect of using different type of amine in the formation of nanorods by keeping the molar ratio of amine-to-acetate at 2. In Figure 5, it can be seen that the alkylamine will affect the dimensions of the nanorods produced. Thus, when dioctylamine (DOA) and hexadecylamine (HDA) were used, nanowires of 26 nm × 500–1500 nm or 37 nm × 200–600 nm were obtained, respectively. When dodecylamine (DDA) was used, however, much shorter and polydispersed nanorods were produced.

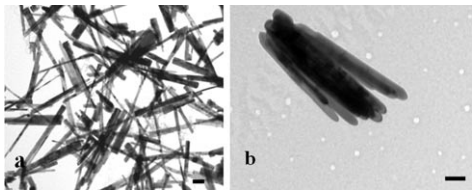

Figure 5. TEM images of one-dimensional ZnO nanocrystals obtained from $Zn(Ac)_2$ reacted with different alkylamine at 240 °C. a) DOA, and b) HDA. The amine-to-acetate molar ratio is kept at 2. Scale bar = 100 nm.

Thus, it seems that longer chain amines will produce thinner (diameter < 50 nm) but longer ZnO nanowires, while shorter chain amines give thicker and shorter nanorods. This

observation may be explained in two ways. On one hand, during the growth process of ZnO nanostructures, longer chain amines could help in the long-range organization of the as-prepared nanorods and hence induced oriented growth in the *c* axis. Similar observation has been reported for the synthesis of cobalt nanowires in the mixture of oleic acid and alkylamine.[15] On the other hand, higher remaining monomer concentration was reported to favor the growth of nanocrystals in the elongated direction.[16]

Control experiments under similar conditions using other capping agent, for example, TOPO or alkanethiol, do not produce ZnO from zinc acetate. Thus, we believe that the decomposition of zinc acetate in our preparation arises from an initial attack of amine onto the carbonyl carbon of the acetate (see below). Since longer chain amines are expected to attack the carbonyl group less readily, higher remaining monomer concentration is expected during the course of nanocrystals growth and growth in the elongated direction is enhanced.

As mentioned earlier, bundles of ZnO nanorods aligned in the same growth direction have been observed as shown in Figures 1a, b, 5a, b, and further in Figure 6. This phenomenon has been described in other reports, which suggested that this could be interpreted as an indication of multiplying growth through the oriented attachment process.[17] The large number of such attachments observed in our case partly reveals the existence of smooth prismatic side planes of the ZnO nanorods. Such observation further confirms the oriented growth process of ZnO nanorods in long chain amines.

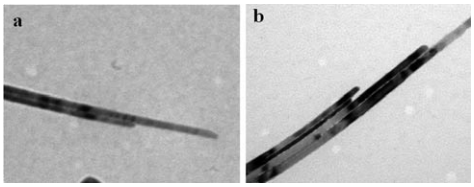

Figure 6. TEM images showing the coplanar growth of a) two ZnO nanorods and b) four ZnO nanorods. These nanorods were prepared with OLA/acetate ratio = 1.

In most reported colloidal synthesis of metal or semiconductor 1D nanocrystals, the anisotropic growth of the 1D structure is often driven by using capping ligands that could bind selectively onto a particular facet of the seed particles.[18] In our case, we observed that addition of more amine would instead impede the unidirectional growth of the ZnO nanorods (Figure 3). This suggests that amine is playing another role as the attacking (or activating) agent, in addition to its capping role. Thus, we propose that the amine molecule may behave like a nucleophile and attacks the electron-deficient carbon of the carbonyl group of acetate as shown in Scheme 1. An addition–elimination process will thus follow to generate the ZnO monomers.

When the amount of amine is decreased, initial nucleation is less and a high remaining monomer concentration is sustained. Since the higher surface energy (002) planes of ZnO nanocrystals will grow faster than the other planes, growth in the elongated *c* axis thus occurs and longer nanowires are produced. When higher concentrations of amine were added, however, nucleation occurs readily and the excess amine would coordinate less selectively with different surface planes of the ZnO nanocrystals. Anisotropic growth along the *c* axis would thus be reduced while growth rates along the *a* and *b* axes would be enhanced.

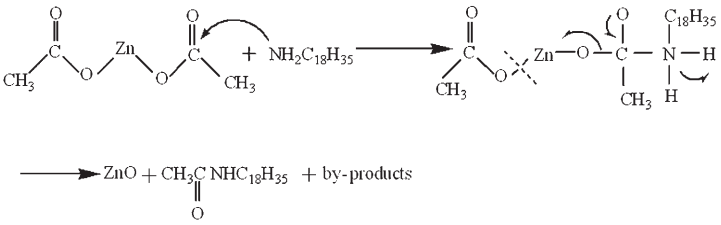

Scheme 1. Proposed reaction mechanism of $Zn(Ac)_2$ with OLA.

In order to elucidate the proposed mechanism, we compared the FTIR spectra of neat $Zn(Ac)_2$ precursor and OLA, with a mixture of $Zn(Ac)_2$ + OLA before and after heating to the reaction temperature (240 °C) as shown in Figure 7 (see Supporting Information S1 for the individual FTIR spectrum for a better view).

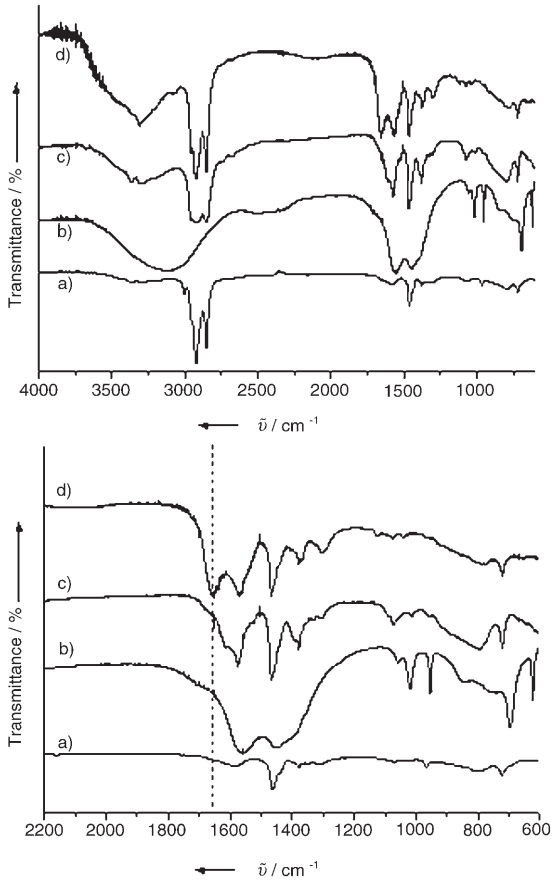

Figure 7. FTIR transmission spectra in the full range (top) and magnified scale (bottom) for a) OLA, b) $Zn(Ac)_2$, (c and d) the mixture of $Zn(Ac)_2$ + OLA at 100 and 240 °C, respectively.

Thus, it was found that the C=O asymmetric stretching mode in $Zn(Ac)_2$ at 1440 cm^{-1} red-shifted slightly by ~15 cm^{-1} when OLA was added at 100 °C. We believe this is an indication of the formation of an intermediate $Zn(Ac)_2$–OLA complex; such red shift can be caused by the donor NH_2 group sharing its lone-pair of electrons with the Zn ions. After heating to 240 °C, a new peak at 1656 cm^{-1} is detected in the reaction mixture. This is attributable to the asymmetric stretching mode of an amide,[19] a side product of the proposed mechanism in Scheme 1. In Figure 8, the NMR spectrum of the reaction residue further confirms the formation of amide by giving a new peak with chemical shift at ~5.8 ppm. This peak is assignable to the -CO-NH proton of N-oleyl acetamide.[19]

The optical absorption and emission spectra (Figure 9) of the prepared ZnO nanocrystals were measured by re-dispersing the samples in toluene. Since both the diameter and length of the triangular nanocrystals and nanorods exceed the Bohr radius of ZnO, it was found that they display similar onset absorption at ~370 nm with tailing to longer wavelength. This spectrum is very similar to those reported in the literature for ZnO nanocrystals prepared by other methods.[10b] (It is believed that the tailing is caused by scattering from the colloidal dispersion, see Supporting Information S2 for the reference UV spectrum of bulk ZnO particles.) The emissive PL spectra of our sample, on the other hand, display a sharp emission at 381 nm with a narrow full width at half maximum (FWHM) of ~20 nm. This can be attributed to the radiative annihilation of excitons.[20] The commonly observed defect peak due to radiative recombination of an electron in the oxygen vacancy with a photogenerated hole[21] is not present in all our samples.

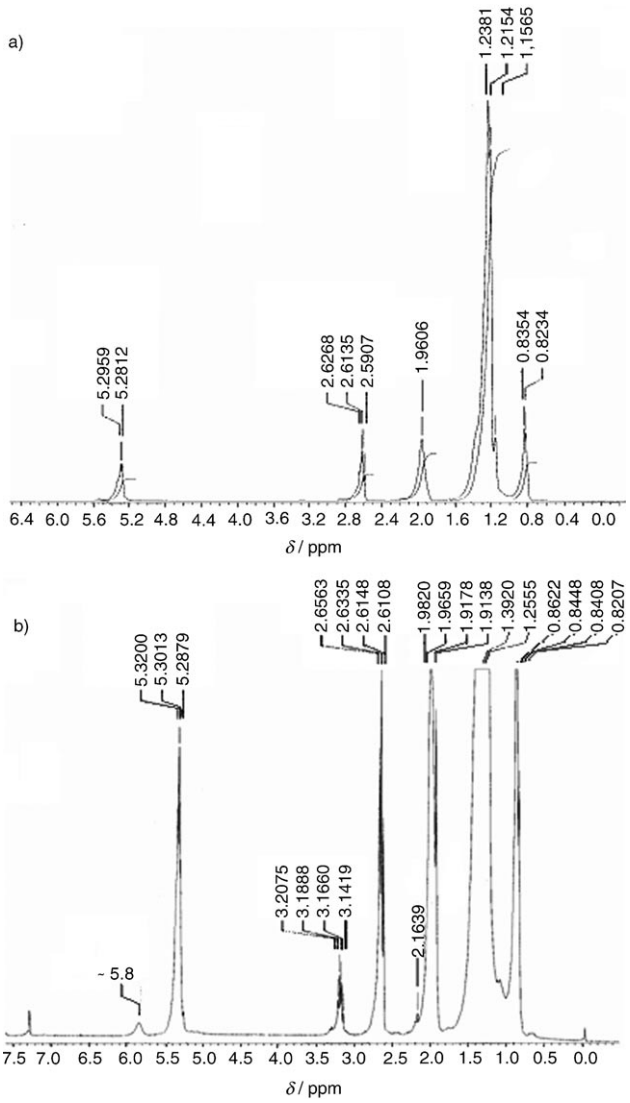

Figure 8. NMR spectra of a) OLA and b) the reaction residue after reaction at 240 °C. Assignment: δ 5.3 ppm -CH=CH; 5.8 ppm -CO-NH; 1 to 2.4 ppm -CH_3 and CH_2 groups. $CDCl_3$ was used as the solvent.

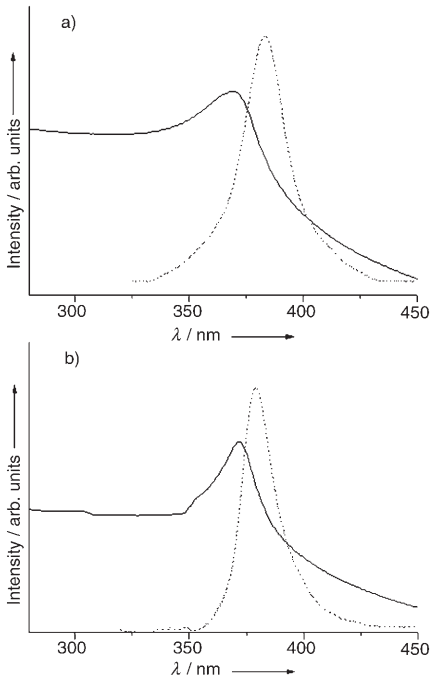

Figure 9. Typical UV/visible absorption (solid line) and PL spectrum (dotted line) of a) triangular ZnO nanocrystals and b) ZnO nanorods. Excitation wavelength for PL = 280 nm.

Conclusion

We have presented above a simple method to prepare ZnO nanocrystals from commercially available acetate by reaction with amine directly. We have also shown that several parameters are important in controlling the size and morphology of the nanocrystals. In order to test the general applicability of our methodology, we have extended our preparation to other types of metal oxide nanocrystals. Three other types of metal oxide nanoparticles have indeed been successfully prepared and the results are summarized in Table 2.

In particular, SnO nanorods (Figure 10) with diameter of ~50 nm and length from 1 to 6 μm were obtained from

Table 2. Morphologies and sizes of various metal oxides prepared from reaction between OLA and the corresponding acetates.

Metal oxide	Precursor	Amine-to-acetate ratio	T [°C]	t [min]	Morphology and sizes
SnO	$Sn(Ac)_2$	12	160	15	rods, 50 nm × 500–1000 nm
CdO	$Cd(Ac)_2$	12	300	30	cubic, ~1000 nm
PbO	$Pb(Ac)_2$	12	280	5	spherical, 20–80 nm

$Sn(Ac)_2$. The good crystallinity of the nanocrystals obtained was confirmed by the XRD patterns which fit well to the tetragonal phase of SnO (JCPDS 85-0712). For the other two metal oxides, CdO and PbO, the XRD patterns also confirm the successful breakdown of the respective acetate by amine to form metal oxides. However, particles with less uniform shapes and sizes were obtained, as amine may not be a good capping agent for the stabilization of these nanoparticles. In these cases, we propose that better quality metal oxide nanocrystals could be obtained by using combination of mixed capping agents, such as TOPO or long chain carboxylic acids.

In summary, we propose a simple and general non-hydrolytic approach to prepare metal oxide nanocrystals. Off-the-shelf metal acetates can be readily used to produce the corresponding oxides in hot alkylamines media. We have found that the reaction conditions for the formation of good quality nanocrystals are particularly easy to optimize using this approach since only two reagents are involved. FTIR and NMR studies have confirmed the production of amide and suggested that amine could mediate a breakdown of the metal acetates, probably through a nucleophilic addition-elimination mechanism. Such a simple synthetic route may possibly be extended to synthesize more complex oxides, such as doped metal oxides or alloys, which have attracted much research attention recently due to their promising applications.

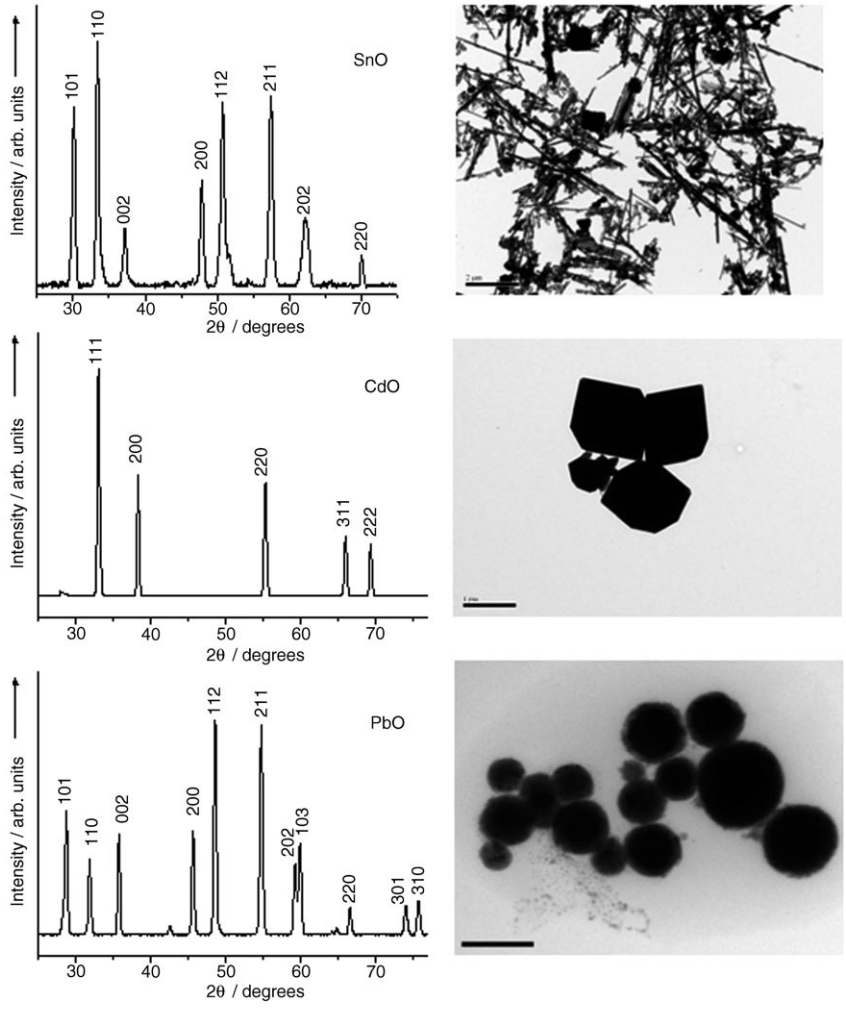

Figure 10. XRD patterns and TEM images of (from top to bottom): SnO nanorods (tetragonal phase, JCPDS 85-0712), scale bar = 2 μm; CdO (cubic phase, JCPDS 75-1529), scale bar = 1 μm; and PbO (tetragonal phase, JCPDS 85-1291), scale bar = 100 nm.

Experimental Section

Chemicals: Zinc acetate (99.9%), tin acetate (97%), cadmium acetate (98%), oleylamine (70%), dodecylamine (99%), dioctylamine (98%) and octylamine (98%) were purchased from Aldrich. Hexadecylamine (99%) and lead acetate (99%) were obtained from Fluka. All manipulations were performed using standard air-free techniques and all chemicals were degassed at 80°C for 1 h under vacuum to ensure that the reaction could be carried out in the absence of oxygen and water.

Synthesis of ZnO nanowires: A typical procedure as follows: First, a stock solution of the precursor was prepared by dissolving $Zn(Ac)_2$ (1 mmol) in oleylamine (OLA, 0.66 (or 0.33) mL; ~2 to 1 mmol) in a three-neck flask. The mixture was degassed with N_2 at 80°C for 30 min and was then quickly heated to 240°C. During the process, the clear yellow solution turned into turbidity and white flocculate appeared. After 20 min, the mixture was cooled down to room temperature. The precipitate was collected by centrifugation at 3000 rpm for 10 min following by washing with ethanol for several times. After vacuum drying, white powders were obtained. For various alkylamines or different molar ratio between zinc acetate and amines, the experimental conditions are similar.

Synthesis of ZnO prism nanocrystals: $Zn(Ac)_2$ (1 mmol) was mixed with OLA (1.33 mL, 4 mmol) in a three-neck flask. The mixture was degassed with N_2 at 80°C for 30 min and was

then quickly heated to 240 °C. After 20 min, the generated white precipitate was collected by centrifugation at 3000 rpm and washed with ethanol for several times. ZnO prism nanocrystals were obtained after vacuum drying.

Synthesis of SnO nanowires and other metal oxides: $Sn(Ac)_2$ (1 mmol) was mixed with OLA (4 mL) in a three-neck flask. The mixture was degassed at 80 °C for 1 h and purged with N_2 three times. The mixture was quickly heated to 180 °C and maintained at this temperature for 30 min. After cooling, the brown precipitate was centrifuged, washed with ethanol and chloroform.

The procedures were similar for the synthesis of CdO and PbO except that the temperature and heating time was at 240 °C and 10 min for CdO, and 300 °C and 15 min for PbO, respectively. Brown powder for CdO and black precipitate for PbO were obtained.

Characterization: UV/Vis and PL spectra were obtained using a Shimadzu UV-1601 spectrometer and a RF-5301 PC fluorometer, respectively. The XRD patterns for the final products were recorded by a Siemens D5005 X-ray powder diffractometer. A JEOL JEM3010 transmission electron microscope (operated at an accelerating voltage of 300 kV) was used to analyze the size, shape, and structure of ZnO nanocrystals deposited on Formvar-carbon-coated copper grids. IR spectrums were recorded using FTS 165 Bio-Rad FTIR spectrophotometer in the range 4000–400 cm^{-1} with KBr or nujol mulls. The ^1H NMR spectrums were recorded on a Bruker ACF 300FT-NMR spectrometer using TMS as an internal reference at 25 °C.

[1] B. O'regan, M. Grätzel, *Nature* **1991**, *353*, 737–740.
[2] J. Karch, R. Birringer, H. Gleiter, *Nature* **1987**, *330*, 556–558.
[3] P. D. Yang, C. M. Lieber, *J. Mater. Res.* **1997**, *12*, 2981–2996.
[4] X. D. Wang, C. J. Summers, Z. L. Wang, *Nano Lett.* **2004**, *4*, 423–426.
[5] R. Skomski, *J. Phys. Condens. Matter* **2003**, *15*, R841–R896.
[6] a) M. Ocana, E. Matijevic, *J. Mater. Res.* **1990**, *5*, 1083–1091; b) M. Ocana, W. P. Hsu, E. Matijevic, *Langmuir* **1991**, *7*, 2911–2916; c) A. Chittofrati, E. Matijevic, *Colloid Surface* **1990**, *48*, 65–78.
[7] a) T. J. Trentler, T. E. Denler, J. F. Bertone, A. Agrawal, V. L. Colvin, *J. Am. Chem. Soc.* **1999**, *121*, 1613–1614; b) M. Niederberger, M. H. Bartl, G. D. Stucky, *J. Am. Chem. Soc.* **2002**, *124*, 13642–13643.
[8] a) S. H. Sun, H. Zeng, *J. Am. Chem. Soc.* **2002**, *124*, 8204–8205; b) S. H. Sun, H. Zeng, D. B. Robinson, S. Raoux, P. M. Rice, S. X. Wang, G. X. Li, *J. Am. Chem. Soc.* **2004**, *126*, 273–279; c) Q. Song, Z. J. Zhang, *J. Am. Chem. Soc.* **2004**, *126*, 6164–6168.
[9] a) W. S. Seo, H. H. Jo, K. Lee, J. T. Park, *Adv. Mater.* **2003**, *15*, 795–797; b) R. Si, Y. W. Zhang, L. P. You, C. H. Yan, *Angew. Chem.* **2005**, *117*, 3320–3324; *Angew. Chem. Int. Ed.* **2005**, *44*, 3256–3260.
[10] a) J. Rockenberger, E. C. Scher, A. P. Alivisatos, *J. Am. Chem. Soc.* **1999**, *121*, 11595–11596; b) P. D. Cozzoli, M. L. Curri, A. Agostiano, G. Leo, M. Lomascolo, *J. Phys. Chem. B* **2003**, *107*, 4756–4762; c) M. Yin, Y. Gu, I. L. Kuskovsky, T. Andelman, Y. Zhu, G. F. Neumark, S. O'Brien, *J. Am. Chem. Soc.* **2004**, *126*, 6206–6207; d) N. R. Jana, Y. F. Chen, X. G. Peng, *Chem. Mater.* **2004**, *16*, 3931–3935; e) J. Park, K. J. An, Y. S. Hwang, J. G. Park, H. J. Noh, J. Y. Kim, J. H. Park, N. M. Hwang, T. Hyeon, *Nat. Mater.* **2004**, *3*, 891–895; f) X. H. Zhong, W. Knoll, *Chem. Commun.* **2005**, 1158–1160; g) S. H. Choi, E. G. Kim, J. Park, K. An, N. Lee, S. C. Kim, T. Hyeon, *J. Phys. Chem. B* **2005**, *109*, 14792–14794.
[11] a) M. Shim, P. Guyot-Sionnest, *J. Am. Chem. Soc.* **2001**, *123*, 11651–11654; b) T. Hyeon, S. S. Lee, J. Park, Y. Chung, H. B. Na, *J. Am. Chem. Soc.* **2001**, *123*, 12798–12801; c) C. G. Kim, K. W. Sung, T. M. Chung, D. Y. Jung, Y. Kim, *Chem. Commun.* **2003**, 2068–2069; d) M. Monge, M. L. Kahn, A. Maisonnat, B. Chaudret, *Angew. Chem.* **2003**, *115*, 5479–5482; *Angew. Chem. Int. Ed.* **2003**, *42*, 5321–5324; e) J. W. Cheon, N. J. Kang, S. M. Lee, J. H. Lee, J. H. Yoon, S. J. Oh, *J. Am. Chem. Soc.* **2004**, *126*, 1950–1951.
[12] a) N. Pinna, G. Garnweitner, M. Antonietti, M. Niederberger, *Adv. Mater.* **2004**, *16*, 2196–2200; b) J. Joo, S. G. Kwon, J. H. Yu, T. Hyeon, *Adv. Mater.* **2005**, *17*, 1873–1877.
[13] Z. H. Zhang, X. H. Zhong, S. H. Liu, D. F. Li, M. Y. Han, *Angew. Chem.* **2005**, *117*, 3532–3536; *Angew. Chem. Int. Ed.* **2005**, *44*, 3466–3470.
[14] a) M. Niederberger, G. Garnweitner, N. Pinna, M. Antonietti, *J. Am. Chem. Soc.* **2004**, *126*, 9120–9126; b) M. Niederberger, N. Pinna, J. Polleux, M. Antonietti, *Angew. Chem.* **2004**, *116*, 2320–2323; *Angew. Chem. Int. Ed.* **2004**, *43*, 2270–2273.
[15] F. Dumestre, B. Chaudret, C. Amiens, M. C. Fromen, M. J. Casanove, P. Renaud, P. Zurcher, *Angew. Chem.* **2002**, *114*, 4462–4465; *Angew. Chem. Int. Ed.* **2002**, *41*, 4286–4289.
[16] X. G. Peng, *Adv. Mater.* **2003**, *15*, 459–463.
[17] a) C. Pacholski, A. Kornowski, H. Weller, *Angew. Chem.* **2002**, *114*, 1234–1237; *Angew. Chem. Int. Ed.* **2002**, *41*, 1188–1191; b) B. Liu, H. C. Zeng, *J. Am. Chem. Soc.* **2003**, *125*, 4430–4431.
[18] a) X. G. Peng, L. Manna, W. D. Yang, J. Wickham, E. Scher, A. Kadavanich, A. P. Alivisatos, *Nature* **2000**, *404*, 59–61; b) N. Cordente, M. Respaud, F. Senocq, M. J. Casanove, C. Amiens, B. Chaudret, *Nano Lett.* **2001**, *1*, 565–568; c) Y. W. Jun, S. M. Lee, N. J. Kang, J. Cheon, *J. Am. Chem. Soc.* **2001**, *123*, 5150–5151.
[19] D. L. Pavia, G. M. Lampman, G. S. Kriz, *Introduction to spectroscopy*, Harcourt College Publishers, Fort Worth, **2001**.
[20] S. Monticone, R. Tufeu, A. V. Kanaev, *J. Phys. Chem. B* **1998**, *102*, 2854–2862.
[21] K. Vanheusden, W. L. Warren, C. H. Seager, D. R. Tallant, J. A. Voigt, B. E. Gnade, *J. Appl. Phys.* **1996**, *79*, 7983–7990.

Received: March 2, 2006
Published online: September 22, 2006

